Exploring the potential of dual-sensitive hydrogels for personalized precision medicine applications

Yi. Xuan Lan a†, Jia. De Yan b†, Hong Lin Su c, Chia Ching Wu d, Chia Hung Kuo e, Chien Chih Chiu f, Ming Wei Chang g, Logan Takemoto a, Ching Chou Wu h i, Hui Min David Wang ajk‡

a Graduate Institute of Biomedical Engineering, National Chung Hsing University, Address: No.145, Xingda Rd., South Dist., Taichung 402, Taiwan, ROC

b Ph.D. Program in Tissue Engineering and Regenerative Medicine, National Chung Hsing University, Taichung City, 402, Taiwan, ROC

c Department of Life Science, National Chung Hsing University, Taichung 402, Taiwan

d Department of Cell Biology and Anatomy, College of Medicine, National Cheng Kung University, Tainan 701, Taiwan

e Department of Seafood Science, National Kaohsiung University of Science and Technology, Kaohsiung 811, Taiwan

f Department of Biotechnology, Kaohsiung Medical University, Kaohsiung 807, Taiwan

g School of Engineering; and Faculty of Computing, Engineering, and the Built Environment. University of Ulster, United Kingdom

h Department of Bio-industrial Mechatronics Engineering, National Chung Hsing University, Taichung City, 402, Taiwan, ROC

iInnovation and Development Center of Sustainable Agriculture, National Chung Hsing University, Taichung City, 402, Taiwan, ROC

j Department of Medical Laboratory Science and Biotechnology, China Medical University, Taichung 404, Taiwan

k Graduate Institute of Medicine, College of Medicine, Kaohsiung Medical University, Kaohsiung 807, Taiwan

Abstract

Background

Melanoma, the uncontrolled accumulation of malignant melanocytes, remains one of the most dangerous and deadly types of skin cancer. Current medical interventions, such as radiation and immunotherapy, are ineffective in treating malignant metastatic melanoma of the lung. Due to the complexity of cancer, abnormalities occur and lead to treatment failure.

Methods

In this study, a novel, dual-reaction hydrogel was composed of a thermo-sensitive type (fundamental) and a pH-sensitive type. In addition, the innovative hydrogel showed thermal reversibility and could liquefy at low temperatures and recover at room temperature. We used

Fourier transform infrared spectroscopy, scanning electron microscopy, thermogravimetric analysis (TGA), and rheometer to observe the hydrogel's mechanical properties.

Significant findings
Results show the hydrogel had a small pore size, revealing positive interactions between molecular chains. The dual-reactive hydrogel exhibited the least cytotoxicity to B16F10 cells *in vitro*, indicating great biocompatibility and potential. The hydrogel in microparticles brings several advantages, including a high surface area-to-volume ratio and delivery within microscale structures. Microfluidic devices are promising for producing hydrogel particles because they enable high-precision flow control during microfabrication, resulting in precise size and shape. This study used a microfluidic device to produce hydrogel particles and encapsulate cells for future drug screening applications.

Keywords: Dual-sensitive hydrogel; Microfluidics; Dielectrophoresis (DEP); Cancer personalized precision medicine

Graphical abstract

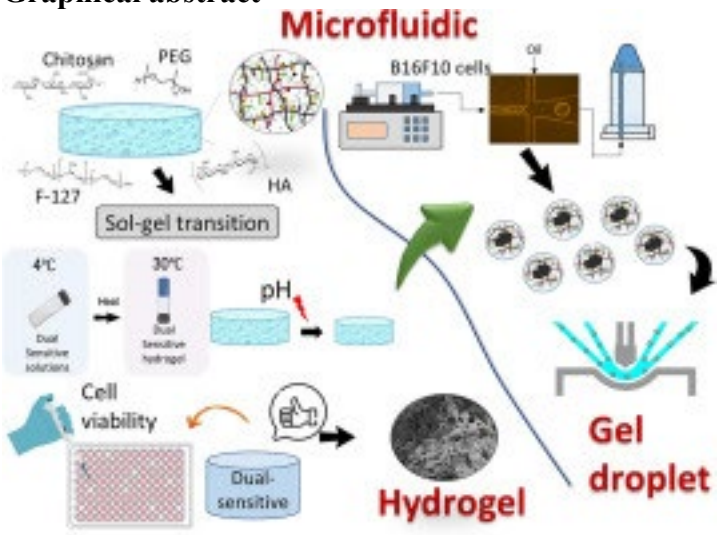

1. Introduction
Skin cancer is considered the one of the most diagnosed cancers in developed and developing countries. Melanoma is a very aggressive skin cancer that seriously threatens human health [1] and is associated with several risk factors, including family history, exposure to certain chemicals, an aging population, and increased UV exposure [2]. It was estimated that about 80 % of skin cancers were caused by melanoma. For patients with metastatic melanoma, the 5-year survival rate was only 5–10 % [3]; however, according to estimates by the World Health Organization (WHO), melanoma incidence and mortality have increased over the past 30 years. There is an urgent need for effective treatments for melanoma, and common strategies for cancer treatment were surgery, chemotherapy, radiation therapy, and immunotherapy, with surgery as the main treatment method for melanoma [4]. Once melanoma was diagnosed, surgical resection was required, but it is considerably more difficult in metastatic melanoma. Treatment outcomes must be evaluated per patient to determine whether the surgical resection was suitable, along with the decision for an appropriate adjuvant therapy. There were only a few treatment options and poor prognoses in the past. For example, melanoma had a low

response rate to chemotherapy of 10-15 %, and treatment was often poorly tolerated [5]. Due to the understanding of melanoma's pathological mechanism, a treatment method targeting the BRAF (V600E) gene had made a breakthrough: about half of melanoma patients had a mutation gene that causes the disease to progress rapidly.

The newly developed targeted therapy uses BRAF small molecule inhibitors, such as vemurafenib and dabrafenib, to inhibit the kinase activity of mutant BRAF and produce rapid tumor suppression. Studies have shown that BRAF inhibits such as dabrafenib improved overall survival in patients with BRAF-mutated metastatic melanoma compared to treatment with dacarbazine in a well-tolerated manner. Another class of targeted drugs developed subsequently were MEK inhibitors [6], such as trametinib and cobimetinib, which could inhibit the MEK's phosphorylation, a downstream transfer factor of BRAF in the MAPK pathway, thereby inhibiting tumor cell growth [7]. With the fast development of cancer immunology in recent years, immunotherapy based on melanoma's mechanism of occurrence and metastasis have become mainstream. The principle of immune cell therapy lay in its identification and tumor cell targeting, different from general chemotherapy drugs or antibody drugs, and have a more precise tumor-killing effect and fewer side effects. However, immune cell therapy often failed to achieve the expected efficacy because cancer cells could escape immune cells through the expression of immune checkpoints such as PD-L1 (programmed death ligand1) and CTLA-4 (cytotoxic lymphocyte-associated antigen 4) [7], therefore preventing immune cells from attacking cancer cells. Taking the earlier CTLA-4 drug (Ipilimumab) as an example, a survey found that in patients with metastatic melanoma, the patients' average survival rate could be extended to about 11 months after accepting immunotherapy [8]. Twenty percent of patients survived for three years or more, and the long-term effects were reassuring. Another report showed that using a PD-1 drug (Nivolumab) was more effective than anti-CTLA-4 drugs, with approximately 30 % of patients surviving for more than five years. However, only 20-40 % of patients reacted to PD-1 therapy.

Hydrogels are hydrophilic three-dimensional network-structured gels with high water content and are flexible analogous to natural tissues [9]. Hydrogels have gained prominence in the last ten years due to their broad range of applications and promising prospects [10]. We used external force to crosslink the polymer, subdivided into physical and chemical crosslinking: physical crosslinking includes hydrogen bonding, ionic interaction, chain entanglement, etc., and chemical crosslinking uses crosslinking agents [11]. We have developed a unique dual-sensitive hydrogel that exhibits thermal sensitivity. This novel hydrogel contained hydrophilic and hydrophobic chemical groups, and the two functional groups could completely react. In a low-temperature environment, the hydrophilic group allowed the hydrogel to expand in the water phase through hydrogen bonds to form a uniform, liquid hydrogel; conversely, if the temperature was higher than 30°C, the hydrogel changed from liquid form to gel phase. The pH-sensitive hydrogel swelled and de-swelled following the pH value shifts. At lower temperatures, the hydrogel can be easily stored as a liquid. As the hydrogel is in contact with the body and increases in temperature, it can change state into a gel, allowing it to conduct its function. pH can also be used to alter the welling of the hydrogel, allowing it to absorb or release its content methodically. This hydrogel could be used for drug transportation or as a biosensor and only required temperature control to adjust the phase transition between liquid and colloidal gel. The phase transition process was reversible to improve the feasibility of clinical applications.

Cancer treatment remained a significant topic. In recent years, cancer treatments have moved towards personalized precision medicine and was currently the director of researchers' efforts

worldwide [12]. In the past, cancer treatment usually used the same set of therapies. However, the same categorical cancer had different genetic mutations, and the therapies applicable to patients should also differ according to the patient status. With the advancement of genetic testing and sequencing technology, according to the tumor genotype, drugs and treatments suitable for different patients could be formulated to find individual differences and optimize the medical process. This was the trend of future medical development. Local treatment strategies have great potential for skin cancers and were superior to traditional treatment modalities. As such, hydrogels were hydrophilic biomaterials that could be fabricated from natural polymers or by various biocompatible syntheses, could be used as drug carriers for skin cancer drug delivery. Drug carriers coated with hydrogels have good biocompatibility, degradability, and low toxicity. In addition, such hydrogel drug carriers were highly desirable to develop a drug delivery system platform for effective cancer therapy. In the future, we could choose the best extracorporeal drugs to avoid wasting medical resources or reduce patients suffering [13].

2. Materials and methods

2.1. Chemicals and reagents

B16F10 melanoma cells (BCRC, Hsinchu, Taiwan) were grown in Dulbecco Modified Eagle Medium (DMEM, Thermo Fisher Scientific Inc., Massachusetts, USA) containing 10 % fetal bovine serum (FBS, Thermo Fisher Scientific Inc., Massachusetts, USA) and 1 % antibiotic antifungal (100X) (Thermo Fisher Scientific Inc.) incubated in a humidified incubator at 37°C and 5 % CO2. The hydrogel manufacturing material was carboxymethyl chitosan (CS), purchased from Biosynth Carbosynth Product Co., Ltd., Switzerland. dimethyl sulfoxide (DMSO), ethylenediaminetetraacetic acid (EDTA), Pluronic F-127 (F127), glyoxal (GX), hyaluronic acid (HA), polyethylene glycol (PEG), and 1,4-butanediol di glycidyl ether (BDDE) was purchased from Sigma-Aldrich Corp., Burlington, NJ, USA. Other chemical reagents and reaction buffers were obtained at the highest available quality levels and purity standards.

2.2. Dual-sensitive hydrogel design

The fabrication process was shown in Fig. 1. CS was dissolved in deionized water, and after stirring, F-127 and the chitosan solution were mixed and stirred for another 30 min at 4°C. Then, GX was added and mixed at 4°C for 10 min, and finally, the hydrogel was formed at 37°C. Since the target temperature for gelation was 30°C, we combined the pH-sensitive hydrogel and mixed the two materials in an appropriate ratio [14]. This hydrogel changed phase in different temperatures and pH. The pH-sensitive hydrogel was prepared as follows: NaOH was used for an alkaline sodium hydroxide solution; then HA and PEG were added, with BDDE as a crosslinking agent. It was mixed at room temperature for 4 h., with a pH of 7.0. The thermo-sensitive hydrogel and pH-sensitive hydrogel were combined at a ratio of 8:2 (v/v).

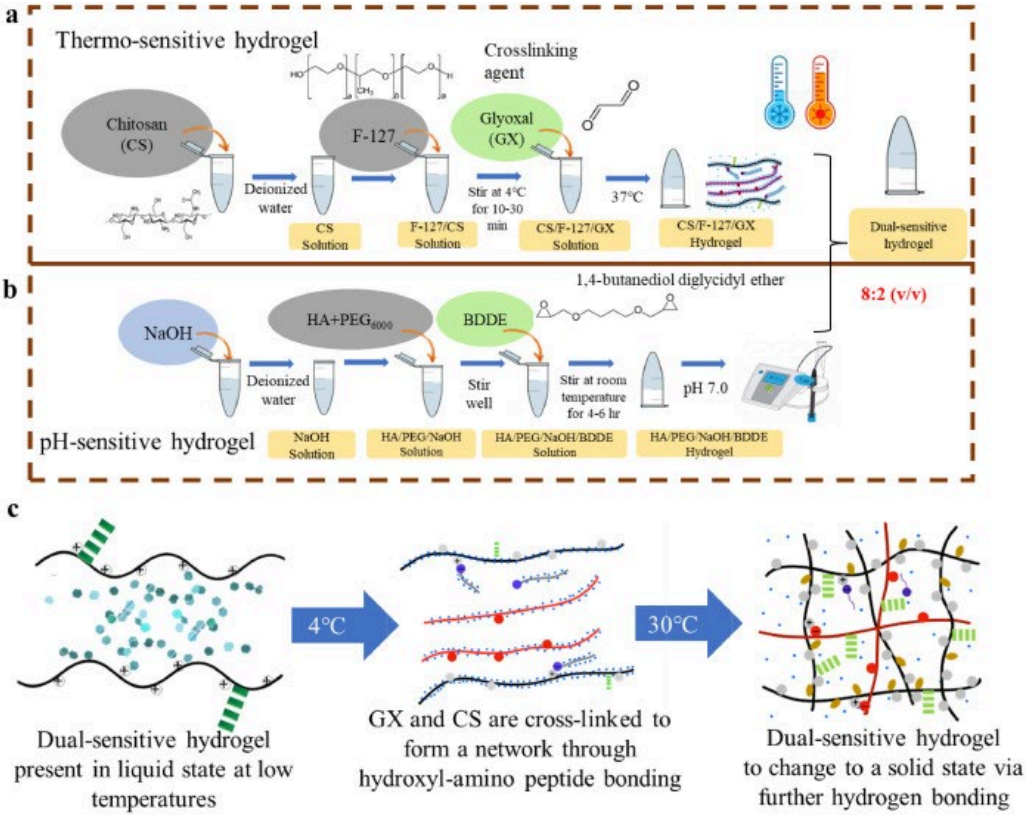

Fig. 1. Chemical synthetic flow chart of the dual-sensitive hydrogel preparation process. (a) CS/F-127/GX thermo-sensitive hydrogel (b) HA/PEG/NaOH/BDDE pH-sensitive hydrogel. The thermo-sensitive hydrogel and pH-sensitive hydrogel were combined at 8:2 (v/v). (c) A demonstration of the state-transition of the dual-sensitive hydrogel across temperatures. As temperature increases past 30°C, Hyaluronic acid and Chitosan form hydrogen bonds, shifting the hydrogel state from liquid to solid.

2.3. Swelling performance (pH issue)

The strong swelling characteristic, which is the most important feature, was measured using the swelling ratio. The hydrogels were placed in solutions at different pH values for 80 min and then weighed. In the study, each sample was analyzed [15]. The following formula was used to calculate the swelling ratio (SR):

$$SR_{pH} = \frac{W_S - W_d}{W_d} \quad (1)$$

where W_d and W_s were, respectively, the mass (g) of the dry gel and the swelled gel.

2.4. Swelling performance (time issue)

To study the swelling performance, the freeze-dried hydrogel samples were put into deionized water, and the liquid on the surface was wiped off with a container for testing immediately. This process was repeated until fully saturated [16].

$$SR_{time} = \frac{W_t}{W_0} \quad (2)$$

where W_t was the swelled sample's weight at time t, and W_0 was the freeze-dried sample's weight.

2.5. Fourier transform infrared spectroscopy (FTIR)

To confirm the polymer-based hydrogels' chemical structure, FTIR tests were performed by a PerkinElmer Spectrum 100 (Thermo Fisher Scientific Inc., Massachusetts, USA) under assay conditions of 4,000-400 cm^{-1} with a resolution of 4 cm^{-1} at room temperature. FTIR spectroscopy of thermo-, pH-, and dual-sensitive hydrogels for functional group identification and spectral signals were utilized to determine interactions between hydrogels.

2.6. Thermogravimetric analysis (TGA)

TGA had a wide range of applications in the ideal temperature range. The species' mass would not change if one species were thermally stable. The TGA curve indicated minimal or no mass loss of significant magnitude. TGA also provided an upper-temperature limit for the substance, beyond which the substance begins to degrade. To determine the samples' thermal stability and physicochemical changes, TGA thermal analysis was performed by a STA6000 (Thermo Fisher Scientific Inc., Massachusetts, USA). A small dry powder (0.5 to 5 mg) was packed in a platinum can. All samples were heated at 10°C per minute under nitrogen, from 35 to 600°C in an isolated environment with purge air. Analysis conditions were 40 mL/min flow rate and heating rate 10°C/min. The results were then plotted with temperature as the X-axis and mass loss as the Y-axis [17].

2.7. Scanning electron microscopic observation (SEM)

Scanning electron microscopy was used to determine the surface pattern. The freeze-dried hydrogel samples were analyzed by ZEISS ULTRA PLUS (Carl Zeiss AG Co., Oberkochen, Germany) at a voltage of 30 kV. The dry area was sliced, and the cross-section was coated with platinum by using a container. The 300 Å gold coating was used to scan the structure, and micrographs were taken of all hydrogel's morphology patch samples [18].

2.8. Rheological measurement

The rheometer was used to analyze the viscoelasticity and gel formation behavior. The hydrogel solution was mixed in a container and put directly on the plate of a Physica MCR 101 rheometer (Physica MCR 101, Austria) [19]. The sample was put in a round container and equilibrated at a particular temperature. The dynamic oscillation mode was used for measurement when the strain was 5 %, which belonged to the linear viscoelasticity range, to reduce the damage to the gel system. In a dynamic temperature scan, the scan time was set to 1000s. During the scan, the instruments were preheated to 37°C, the frequency was set to 10 rad/s, and the temperature increased at a rate of 2.5°C/min from 10 to 45°C [20]. The hydrogel solution was then delivered to the plate and placed on the plate for the 30s to scan.

2.9. Cell viability examination

The 3-(4,5-dimethylthiazol-2-yl)-2,5-diphenyl-2H-tetrazolium bromide (MTT) test should be used for judgment. Hydrogels are widely used materials, and their biocompatibility must be studied. The prepared hydrogels were placed in a 96-well plate and sterilized before placement. The absorbent OD_{Blank} value at 570 nm was measured using an enzyme-linked immunosorbent assay. After 24 hr, the wells were washed with phosphate-buffered saline (PBS). The number of cells required for the experiment was calculated, and melanoma cells (1×10^4 cells/mL) were inoculated in 96-well plates. Then, the cells were inoculated in 96-well plates and cultured in a CO_2 incubator for 24 hr. All the culture medium was aspirated, and 90 μL of the medium without serum and 10 μL of MTT solution were added to each well. Incubation continued for 4 more hours to form formazan, then liquid was removed from wells, and DMSO solution (100

μL) was added to each well. With a microplate reader, wells were shaken for 5 min, and absorbance was measured at 570 nm [21]. The cell survival rate was calculated as follows:

$$\text{Cell viability} = \frac{A_{Sample} - A_{Blank}}{A_{Control} - A_{Blank}} \times 100\% \quad (3)$$

The A_{Blank} was the absorbance of untreated cells, A_{Sample} was the absorbance of the sample used, and A_{Control} was the absorbance of cells inoculated without treatment.

2.10. Microfluidic system Design

The droplet microfluidic system utilized two distinct phases of a liquid (gel/oil) to generate droplets by pinching in microchannels. Each microbead could be regarded as a microreactor. Magnetic beads could contain cells and drugs for cell proliferation, differentiation, co-culture, gene transfer, dynamic enzymatic reactions, or drug screening tests (Fig. 2a). Additionally, microchannels for droplet generators and droplet sorters were designed in this study. Afterward, the two chips were fabricated by photolithography and flipped with polydimethylsiloxane (PDMS), as shown in Fig. 2b. Cancer cells in the hydrogel will be injected into microchannels to create droplets [22] (Permission from Prof. Ching-Chou Wu's lab).

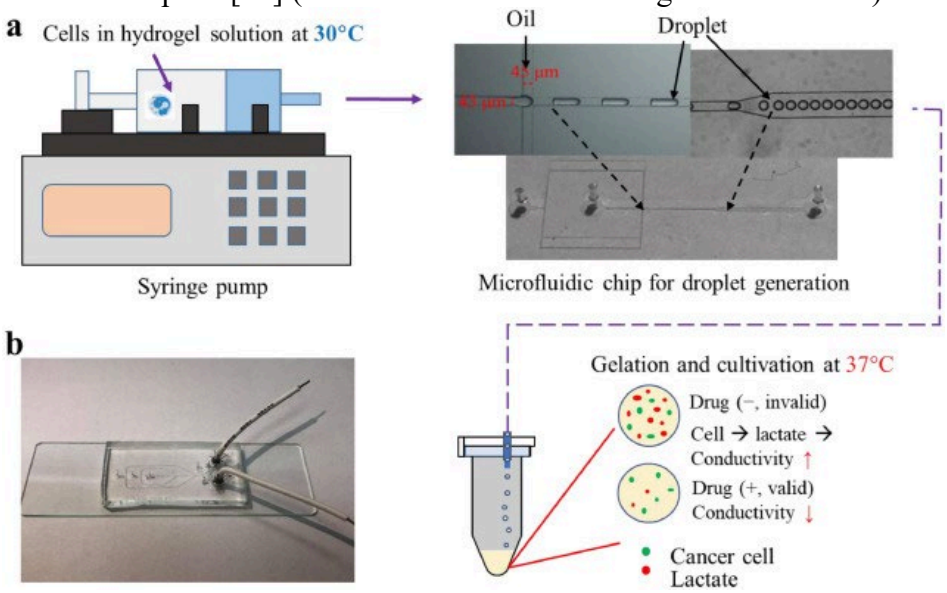

Fig. 2. (a) The droplet generation system for the entrapment of a single cell or droplet. Left: syringe pump and microfluidic chip for droplet generation. (b) The microchannel chip with 3D electrodes for droplet sorting.

2.11. Statistical analysis

Analytical comparisons were expressed as mean ± standard deviation, completed in triplicate, while significance is expressed as $P< 0.05$*, $P < 0.01$**, $P < 0.001$***, respectively. Differences between two groups were compared using a student's t-test for multiple values, while comparisons between three or more groups were completed using an ANOVA analysis.

3. Results and discussion

3.1. Dual-sensitive hydrogel swelling performance

Hydrogel capability at different pH values in buffer solutions of 2.0, 4.0, 6.0, 7.4, 8.0, 10.0, and 12.0 were determined. 0.2 g of hydrogel was taken and placed it in buffer solutions (50 mL) of differing pH values for 80 min, then filtered and weighed after absorbing water.

According to the hydrogel's formula, the water absorption rate at different pH values was calculated. As shown in Fig. 3a, the degree of swelling of the dual-sensitive hydrogel in water increased with increasing pH. This was because a dissociative complex was shaped between hyaluronic acid and polyethylene glycol with changes in pH. In a low pH environment, carboxyl groups on hyaluronic acid and the ethoxy bunches on polyethylene glycol form hydrogen bonds to shape a complex, bringing about diminished solvency in water and precipitation; if the solution pH value increased, hyaluronic acid ionized at this point, separating from polyethylene glycol, and the two re-dissolved in water. To know the hydrogel's water absorption capacity, the swelling ratio (SR) was tested to determine the swelling performance [23]. Fig. 3b showed the SR value of the prepared dual-sensitive hydrogel over time. The dual-sensitive hydrogel exhibited a good swelling reaction- whereas as time increased, the hydrogel's swelling ratio gradually increased relatively porportionally to it's time in water. This phenomenon occurred as water was easily diffused into the hydrogel network, leading to relatively rapid swelling in the hydrogel network. It is to be expected that the hydrogel will reach a saturated state to balance the swelling with additional time in water.

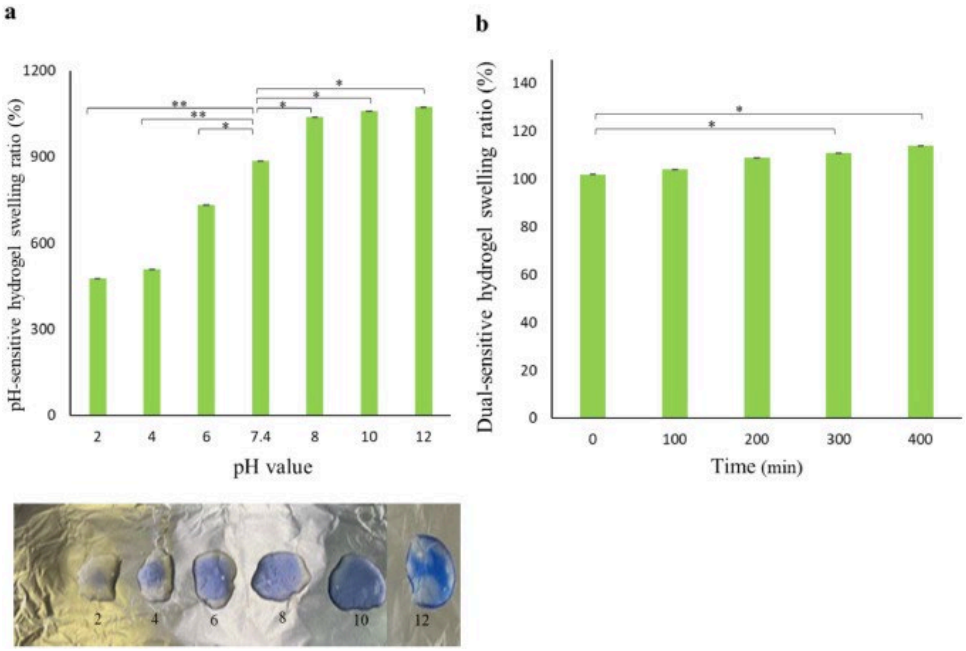

Fig. 3. The swelling ratio of the dual-sensitive hydrogel. (a) The hydrogel swelling rate post-treatment from different pH buffer solutions for 80 min. The hydrogels dyed blue demonstrate swelling at various pH ratios. (b) To investigate the swelling performance, the freeze-dried hydrogel samples were immersed in deionized water and evaluated immediately after liquid removal on the gel surface using a wet sponge. Data are presented as the mean ± SD. *$P < 0.05$, and ** $P < 0.01$ by the t-test.

3.2. FTIR analysis

FTIR spectroscopy analyzed the hydrogel's chemical structure. The characteristic absorption signals of all hydrogels were observed in the FTIR spectra of three different hydrogels (Fig. 4a), which confirmed the existence of dual-sensitive hydrogel in the thermo-sensitive and pH-sensitive hydrogel. In addition, the FTIR spectrum of dual-sensitive hydrogel showed OH tensile vibration at 1466.95 cm^{-1} and CH bending at 841.96 cm^{-1}, indicating that dual-sensitive hydrogel had thermo-sensitive characteristics. Dual-sensitive hydrogel showed OH tensile vibration at 2883.27 cm^{-1} and CH bending at 962.71 cm^{-1}, indicating that dual-sensitive hydrogel had pH characteristics. It was proven that dual-sensitive hydrogel had the

characteristics of a double reaction, and it could be observed that it shared many thermo-sensitive characteristics similar to it's products. The thermo-sensitive hydrogel's composition accounted for 80 % of the dual-sensitive hydrogel.

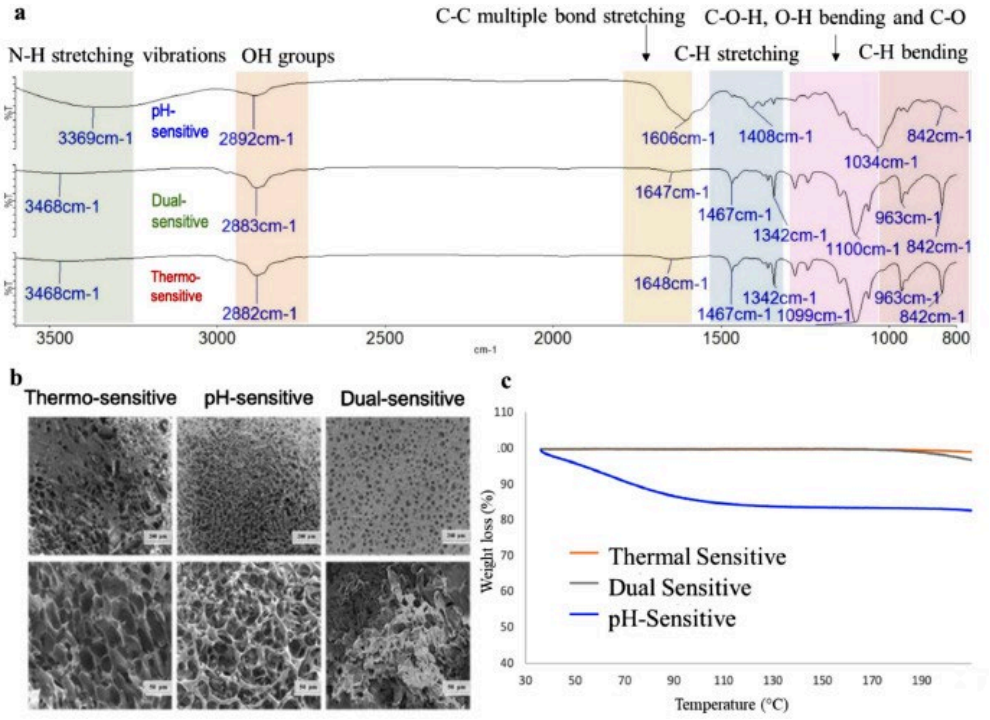

Fig. 4. (a) Dual-sensitive hydrogels were analyzed chemical structure by FTIR spectrometer in transmission mode. The sample is scanned from 400 cm^{-1} to 4000 cm^{-1} with a resolution of 4 cm^{-1} for characterization. (b) Thermo-, pH-, and dual-sensitive hydrogels were used to observe the cross-sectional morphology of freeze-dried samples by SEM at an accelerating voltage of 30 kV. (c) The thermal stability of three hydrogels were measured by TGA under a nitrogen atmosphere at a heating rate = 10°C/min^{-1}, at 35 to 600°C.

However, the gelation time was significant for biomedical applications, and the tube inversion method was the method for recording the gelation time. As previous reports suggested, the gelation time of a hydrogel with a single cross-linking method has been established to be relatively long. To improve this situation, the crosslinking density of the hydrogel was increased by adding a crosslinking agent. The swelling ratio of the hydrogels was measured in deionized water at room temperature at different time intervals. The hydrogels all had good swelling properties, attributed to their higher crosslink density. FTIR confirmed the dual-sensitive hydrogel's chemical structure, and the characteristic peaks denoting functional groups in themal and pH sensitive gels were shared with the novel dual-sensitive gel, indicating that the dual-sensitive hydrogel had characteristics of both. The hydrogel was additionally surveyed by scanning electron microscopy, and the hydrogels were found to display porous structures. The pore size of the dual-sensitive hydrogels was smaller than that of the thermo-sensitive and pH-sensitive gels. due to the increased crosslink density and tight intermolecular bonding in the hydrogels.

3.3. Hydrogel morphology

To observe the hydrogel's shape, it was freeze-dried in a lyophilizer for 24 hr. Furthermore, the cross-sections were coated with platinum. Fig. 4b showed the SEM observation results [24].

Respectively representing thermo-sensitive, pH-sensitive, and dual-sensitive hydrogels, all hydrogels were found to have porous structures. The dual-sensitive hydrogel had a smaller pore size than the other two hydrogels. Changes in internal molecular interactions may have caused these changes. HA and CS contained carboxyl and amino groups. According to the literature, a potential hydrogen bond existed between the carboxyl and amino molecules, and HA cross-links with CS, revealing good interactions between HA and CS molecular chains [25].

3.4. TGA analysis

Thermogravimetric analysis, TGA, was a technique for evaluating the thermal stability of materials. If a certain species was thermally stable within the required temperature range particular, no mass change will be observed. The minimal mass loss had only a small change or no amplitude in the TGA curve. The hydrogel's TGA was shown in Fig. 4c, and the TGA curves of the dual-sensitive hydrogels exhibited higher decomposition temperatures, indicating that the thermal stability of the dual-sensitive hydrogels was higher than that of the thermo-sensitive hydrogels and pH-sensitive hydrogels. The thermo-sensitive and dual-sensitive hydrogel had only minimal changes in the TGA curve, indicating that the sample weight remains unchanged. However, the pH-sensitive hydrogel significantly dropped at 35°C, and the weight loss tended to be stable after 70°C. This result could also have represented that the dual-sensitive hydrogel was composed of thermo-sensitive and pH-sensitive hydrogel, with the thermo-sensitive hydrogel accounted for a more significant proportion. Dual-sensitive hydrogel was composed more similarly to thermo-sensitive hydrogel and the results were consistent with the FTIR. Considering that the ideal gelation temperature is between 25-37°C for biomedical applications, the the dual-sensitive hydrogel remained stable considerably past 37°C, up to approximately 190°C. The results support that the dual-sensitive hydrogel had no obvious toxicity to cells through deterioration at high temperatures.

3.5. Rheology property

Gel temperature was an important parameter for gel formation, especially in hydrogel systems. The gelation temperature was also known as the phase transition temperature at which the liquid phase transforms into the gel phase. The ideal gel temperature for biomedical applications should be between 25-37°C; the dual-sensitive hydrogels exhibited specific transitions in the LCST transition from liquid to gel. This study determined the gel temperature at the temperature at which the G' (storage modulus) and G" (loss modulus) curves overlapped. To check whether the hydrogel could be used clinically, the storage modulus (G') and loss modulus (G") were measured to demonstrate its viscous behavior [25]. When the hydrogel was in liquid form, G' was relatively small. When gelling occures, during crosslink, G" increased suddenly. The gelation temperature was defined as G' equals G". As shown in Fig. 5a, it could be observed that, compared with thermo-sensitive (37.2°C), the dual-sensitive gel temperature decreases with the increases of HA content. That was, thermo-sensitive: 37.2°C, pH-sensitive: 37.1°C, dual-sensitive: 31.2°C; the introduction of HA promotes an overall decrease in gelation time while remaining in the optimal 25-37°C range. The shear strain (γ) scanning test shows that when the strain was less than 0.3 %, the gel had a viscoelastic response (Fig. 5b). Within the measured strain range, the storage modulus (G') was always greater than the gel loss (G"). The factor (tan δ) was less than 0.06, indicating that the gel was elastic. (Fig. 5c). G' increases slightly as the frequency increases, and then G' first decreases and then slightly increases, so there was a minimum tan δ at 10 rad s−1, possibly due to the breakdown of the balance among hydrogen. The hydrogel's viscoelastic behavior confirms its excellent stability and elasticity [26].

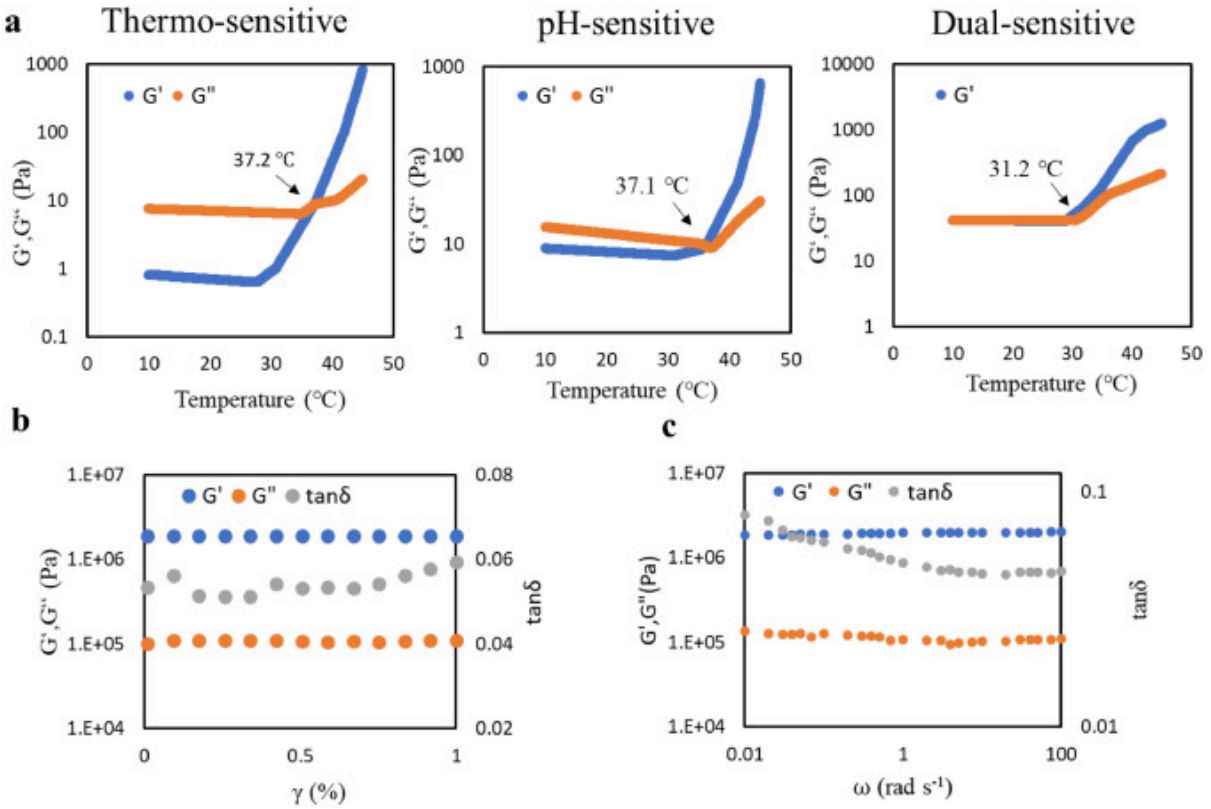

Fig. 5. Thermo-, pH- and dual-sensitive hydrogels were used DHR-2 stress-controlled rheometer for dynamic temperature scanning test (a) Rheology measurement of the hydrogel. Storage modulus (G'), loss modulus (G"), and loss factor (tan ϴ) are functions of (b) shear strain and (c) frequency.

In this study, we designed a dual-sensitive hydrogel with temperature and pH phase transitions; the hydrogels exhibited good mechanical properties. In this work, F127 was selected as the main material for the hydrogel, a synthetic biocompatible hydrogel widely used for drug delivery and controlled release. It had extraordinary properties of injectable hydrogels, resembling the extracellular matrix in natural tissues, and was fabricated without toxic cross-linking agents. Despite the potential advantages of F127 hydrogel in biomedical applications, its poor mechanical properties required the design of a new type of hydrogel material. While gelation time was important for biomedical applications, F127 endowed the hydrogel with thermal sensitivity. At the same time, while CS increased the gelation temperature, GX, in turn, enhanced the wholeness of the hydrogel, making the hydrogel insoluble in the medium. The micellization of F127 was broken by CS, so the gelation temperature of F127/CS/GX was higher than that of pure F127, which ranged from 21 to 29°C dependent on hydrogel concentrations [27]. In this work, CS acted as chitosan to break the F127 gelation. Finally, the amino groups of GX and CS were cross-linked to form a network. The hydrogel remained whole in the aqueous environment due to the interaction between its hydroxyl and amino groups. This formed a protonated amino group. When we added HA, the carboxyl moiety of the HA molecule neutralized the protonated amino group, resulting in a decrease in the repulsive force between the CS molecules. While CS, HA, and PE G were rich in hydrophilic groups, which could form hydrogen bonds with water molecules, the electric attraction between NH3+ of CS and COO− of HA also reduced the electrostatic repulsion. With the increase in temperature, hydrogen bonds were formed between CS and HA (Fig. 1c). The enhanced

interaction between HA and CS enhanced the hydrogel's mechanical strength, shortened the gelation time, and resulted in a denser structure of the hydrogel.

3.6. Biocompatibility

A good material must be highly biocompatible, and the results support that the dual-sensitive hydrogel had no obvious toxicity to cells through deteriorations. The dual-sensitive hydrogel was tested for cell viability with B16F10 cells. The cell survival rate was observed in the hydrogel environment, more than three independent sample examinations were used, and the control group was blank. Photos were observed at 12 and 24 hr, respectively, and the cell survival rate was not affected by different concentrations of hydrogel growth environment, as shown in Fig. 6a. In the future, we plan to measure various test cells further. Biocompatibility was essential for determining the scaffold material, distinguished by cell survival. To study the dual-sensitive hydrogel's biocompatibility, a cell viability assay was performed to represent the cell viability of B16F10. As shown in Fig. 6b. The hydrogel did not produce apparent cytotoxicity over time, indicating that the dual-sensitive hydrogel had good biocompatibility [28].

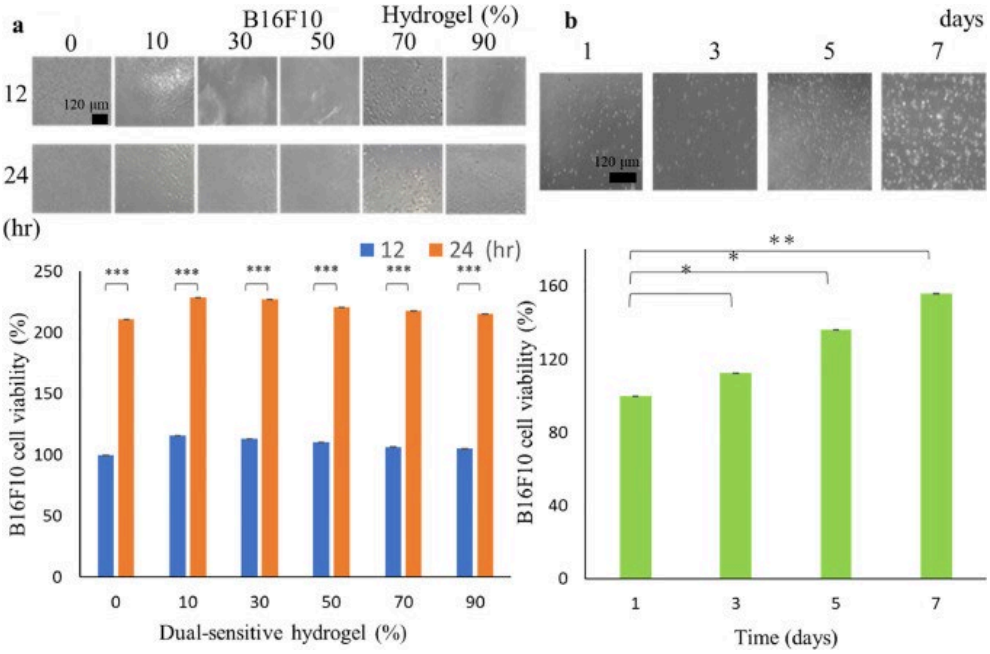

Fig. 6. (a) The survival rate of B16F10 cells at ■12 and ■24 hr under different concentrations of hydrogel growth environment for melanoma cells. We confirmed that different hydrogel ratios do not affect the cell survival rates. (b) The survival rate of B16F10 cells at 1, 3, 5, and 7 days under a dual-sensitive hydrogel growth environment for melanoma cells. Data are presented as the mean ± SD. *$P < 0.05$, ** $P < 0.01$, and *** $P < 0.001$ by the t-test.

In recent years, the development of clinical applications for cancer treatment has sprung up to improve cancer outcomes. The accumulation of evidence from clinical trials and the gradual understanding of tumor heterogeneity showed that cancer treatments with a single target as the treatment orientation were no longer the optimal strategy for cancer treatment. Case in point: dual immune checkpoint blockade (ICB) with ipilimumab-nivolumab improved response rates in metastatic melanoma patients (58 % response rate) compared to single-agent ipilimumab or nivolumab [29]. BRAF and MEK inhibitor combination therapies were more effective than BRAF inhibitors alone, allowing more patients with metastatic melanoma to achieve a 12-month survival time [30]. Additionally, Opdualag recently received FDA approval for the

treatment of melanoma. Opdualag comprised a novel LAG-3 monoclonal antibody, relatlimab, and a PD-1 inhibitor, nivolumab. Opdualag was the first approved cancer treatment regimen containing a LAG-3 inhibitor, with a survival rate of 47.7 % [31], indicating that combination therapy was a promising cancer treatment strategy. Currently, immunotherapy, combination therapy, local therapy, and targeted therapy strategies are commonly used in clinical cancer treatment [3]. Among them, multiple works of literature show that topical therapy effectively improves cancer treatment, with hydrogel as one potential topical strategy [32]. The hydrogels as targeted drug delivery platforms had shown great potential in localized cancer therapy.

3.5. Optimization of the microfluidic system and dual-sensitive droplet

In addition to study on hydrogel characteristics, the microfluidic system was optimized. As noted in Section 2.10., the microfluidic design involves running liquid hydrogel containing viable carcinomic cells across a perpendicular pipe depositing oil to “pinch” the continuous steam of hydrogel into indivisual microspheres of hydrogel, each containing a few cells (Fig. 2a). The intention of the design involves the creation of muiltiple small scale cancer cell environments in each hydrogel, providing the ability to measure and test drug effectiveness with limited cells prior to committment to a specific drug treatment.

The microfluidic system's advantages were: First, hydrogel viscosity to keep cell suspension feasible for controlling the cell density during droplet generation under the Tm point [33]. Second, gelation droplets were suitable for cell-laden cultivation and the performance of anti-cancer drugs susceptibility tests; we used the concept of oil-water separation to form droplets (Fig. 7a). The results showed that the droplet size produced by 10 % hydrogel at different flow rates, the higher the colloid flow rate, the larger the droplet size (Fig. 7b). However, at a fixed flow rate of 100 μL per hr, different hydrogel concentrations changed the diameter of the droplet due to the viscosity system. At 10 %, it had 86 μm, high colloidal viscosity, and small droplet size (Fig. 7c). For a bead cells dispersion, a density of 15-20 million cells fell between 3-7 beads (Fig. 7d). We also used jc1 to observe the cell activity by culturing the cell-laden droplet for 1 hr, finding that the cells in the droplet did not lose cell viability (Fig. 7e).

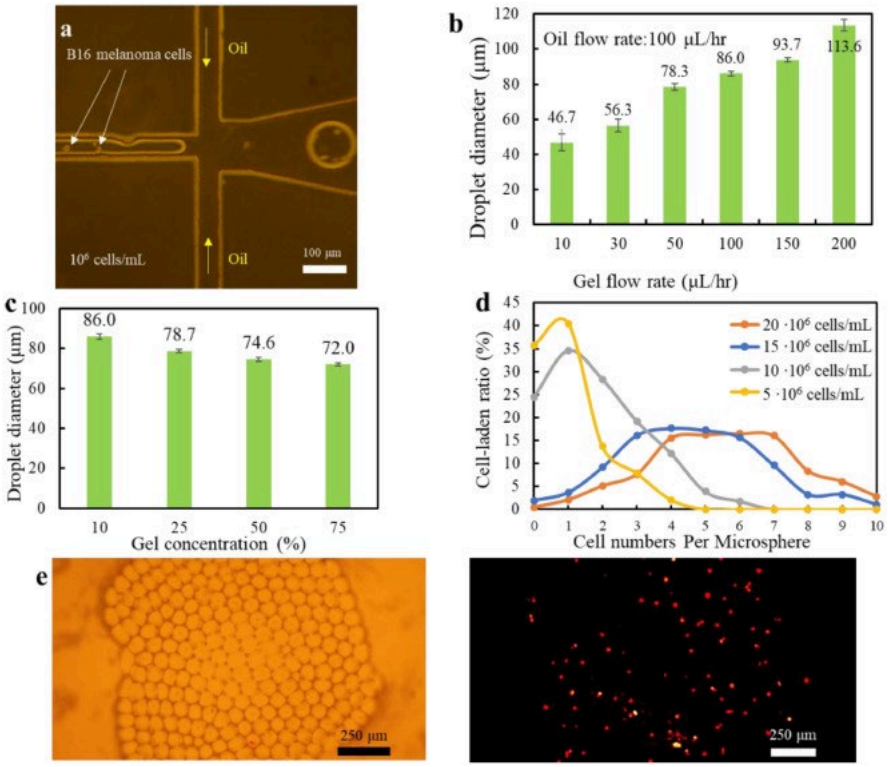

Fig. 7. (a) Microchannels for focusing flow. (b) Droplet sizes were produced by a different flow rate of 10 % gel. (c) The droplet size of the concentration-varied gel was made at a 100 μL/hr rate. (d) Cell number distribution per gel droplet via variable cell flow rates (e) JC1 staining was used to observe the cell viability of cell-laden droplets cultured for 1 hr. Data are presented as the mean ± SD.

Melanoma, the uncontrolled accumulation of malignant melanocytes, is one of the most dangerous and deadly skin diseases, with obstacles in treating malignant metastatic melanoma of the lung. To improve cancer treatment effectiveness, the current treatment trend is using precision medicine to discover individual differences and optimize medical procedures [34]. In short, by sequencing the genes of normal people and individual cases, comparing and analyzing diseases, and using targeted drugs, cell therapy, and other treatments to fight viruses or genes precisely, cancers could be cured safely and effectively. Unfortunately, precision medicine was still not completely effective in treating cancer, with even less than 50 % effectiveness (current PD-1/PDL-1 antibody therapy); for example, melanoma occurs mainly due to BRAF gene mutation, but about half of the patients were insensitive to BRAF inhibitors, leading to poor treatment outcomes. If a patient's genetic sequence was tested before administration, it could detect whether a patient had a mutation in a particular gene. However, due to the complicated nature of cancer, there were often no known cancer gene mutations at the point of the mutation, nor corresponding drugs with garenteed effectiveness. In this case, the treatment selection could only rely on the doctor's expertise and prior experiences. Although many drugs had great clinical benefits for the treatment of melanoma, patients were still very troubled by side effects. The patient and the doctor must discuss how to strike a balance between side effects and treatment effectiveness and whether the patient's prognosis could receive the proper care. Ineffective radiotherapy, surgery, chemotherapy, or immunotherapy treatment was the current obstacle to treating malignant metastatic melanoma. Despite the rapid development of precision medicine, there were still the following challenges: (1) The long experiment time drags down the disease development. (2) It requires a lot of experimental consumables and is expensive. (3) Huge number of personnel was required. (4) Monitoring and measuring

immediately after the medication was impossible. The key to the above reasons was that the current cell viability assay technology after drug use required at least 2,000 cells to be detected by existing detection systems, and the dyes used were expensive and could not be reused [35].

To remedy this problem, we adopt a microfluidic droplet system by using two different phases of liquid fluids (gel/oil) to generate droplets in a microfluidic channel; each droplet could be regarded as a microreactor. Droplets could contain cells and different drugs for experiments such as cell proliferation, differentiation, co-culture, or drug screening on a small scale. The volume of a single droplet was small, and the required number of test cells and drug dosage requirements were far lower than the traditional 96-well plate test method, which are characteristics attractive to precision medicine. Therefore, we designed novel dual-sensitive hydrogel beads using a microfluidic system incorporating flow channels. Using micro-electromechanical technology to make tiny flow channels and valves into a droplet sorting system, the huge and complicated analysis system could be miniaturized to a wafer of only a few centimeters squared to realize the concept of a miniature full analysis system. The development of digital fluid technology provided a method for effectively driving micro-beads, which greatly improved the performance of microfluidic systems. These microdroplet systems could drive tiny droplets 1000 times to 1 million times smaller than traditional dropper methods to encapsulate skin cancer cells (B16F10) to produce hydrogel particles for future drug screening applications. As a microenvironment composed of cancer cells, this miniature full analysis system allows for possibility of a drug effectiveness assay with a limited sample of personal carcinogenic cells.

The dual sensitive hydrogel demonstrated strong biocompatibility with B16F10 cells, allowing this hydrogel to be a strong candidate for the base hydrogel for microdroplet formation. As seen in Fig. 6, B16F10 cells were able to survive within the hydrogel environment, regardless of hydrogel concentration or time. Additionally, the dual sensitive hydrogel has been tested with variable settings with the microfluidic system (Fig. 8); altercations to the cellular flow rate, hydrogel concentrations, and gel flow rate have demonstrated variable changes to droplet diameter as well as cell numbers per droplet. The data from Fig 8 suggests the capability of altering cellular flow rate, gel flow rate and hydrogel concentrations to adjust the specifications of created microsphere as needed.

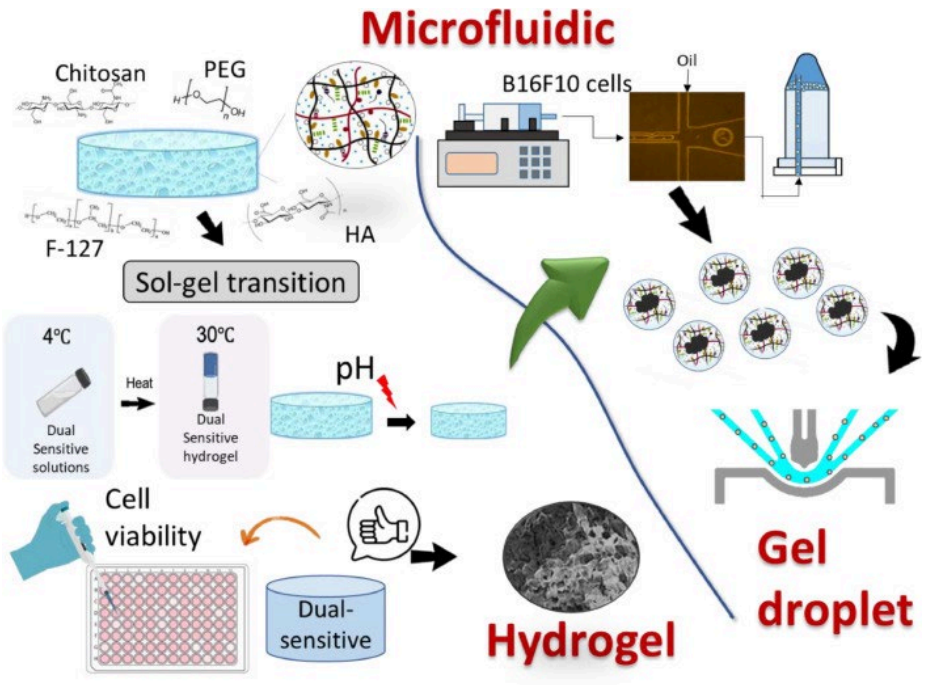

Fig. 8. The schematic illustration of the rapid estimation platform for anticancer drugs established using dual-sensitive hydrogel embedding technology.

As noted above, the main concern involved in many drugs designed to treat melanoma is the large variability in effective treatment across patients. Determining the most effective treatment plan for each patient efficiently is crucial considering the lethality and difficulty of treating cancers such as melanoma. With this method, even skin biopsies could potentially be sampled to assist in determining the most effective treatment method prior to beginning the treatment plan, eliminating any trial-and-error period for treating aggressive cancers.

4. Conclusions

In conclusion, a novel dual-sensitive hydrogel was prepared with both temperature and pH phase change (gel/water) properties. The mechanical properties indicated that the hydrogel had a good swelling ratio and a small pore size. In addition, the use of cell viability assays to show that the hydrogel provided a good biological cell environment supports a system that better simulates *in vivo* conditions when combined with a microfluidic system to affect skin cancers (B16F10) in three dimensions, establishing a system that did not require antibody calibration and fluorescence. Finally, in conjunction with developing the unique hydrogel, a microfluidic system suitable for cell-laden cultivation and the performance of anti-cancer drug susceptibility tests was established. In the future, cancer cells containing anticancer drugs could be encapsulated in hydrogels to form droplets for droplet sorting. After optimizing all parameters, the establishment of a rank ratio index can serve to evaluate the efficacy of candidate anticancer drugs (Fig. 8).

Declaration of Competing Interest

The authors declare that they have no known competing financial interests or personal relationships that could have appeared to influence the work reported in this paper.

Acknowledgments

This research was supported by the Ministry of Science and Technology (MOST), Taiwan under grant nos. MOST 111-2221-E-005-026-MY3, 111-2221-E-005-009 and 110-2221-E-029-005.

References

[1] Cheng YC, Chang YA, Chen YJ, Sung HM, Bogeski I, Su HL, et al. The roles of extracellular vesicles in malignant melanoma. Cells 2021;10(10):2740.
[2]Marzi M, Rostami Chijan M, Zarenezhad E. Hydrogels as promising therapeutic strategy for the treatment of skin cancer. J Mol Struct 2022;1262:133014.
[3] Chen CY, Kuo PL, Chen YH, Huang JC, Ho ML, Lin RJ, et al. Tyrosinase inhibition, free radical scavenging, antimicroorganism and anticancer proliferation activities of Sapindus Mukorossi extracts. J Taiwan Inst Chem Eng 2010;41(2):129–35.
[4] Davar D, Tarhini AA, Kirkwood JM. Adjuvant therapy in melanoma. Emerg. Therap. Melanoma 2012:58–79.
[5]Mdlovu NV, Lin KS, Chen Y, Juang RS, Chang TW, Mdlovu NB. Formulation and characterization of multifunctional polymer modified-iron oxide magnetic nanocarrier for doxorubicin delivery. J Taiwan Inst Chem Eng 2020.
[6] Hedayat M, Jafari R, Majidi Zolbanin N. Selumetinib: a selective MEK1 inhibitor for solid tumor treatment. Clin Exp Med 2022;23(2):229–44.
[7] Lugowska I, Teterycz P, Rutkowski P. Immunotherapy of melanoma. Wsp´ołczesna Onkologia 2018;2018(1):61–7.
[8] Vanella V, Festino L, Vitale MG, Alfano B, Ascierto PA. Emerging PD-1/PD-L1 antagonists for the treatment of malignant melanoma. Expert Opin. Emerg. Drugs 2021;26(2):79–92.
[9] Sabbagh F, Muhamad II. Acrylamide-based Hydrogel Drug Delivery Systems: Release of acyclovir from mgo nanocomposite hydrogel. J Taiwan Inst Chem Eng 2017;72:182–93. Fig. 8. The schematic illustration of the rapid estimation platform for anticancer drugs established using dual-sensitive hydrogel embedding technology. Yi.X. Lan et
al.
JournaloftheTaiwanInstituteofChemicalEngineersxxx(xxxx)xxx 11
[10]Wang TC, Tsai WB. A biphasic mathematical model for the release of polymer-drug conjugates from poly(vinyl alcohol) hydrogels. J Taiwan Inst Chem Eng 2022;135: 104395.
[11] Cao H, Duan L, Zhang Y, Cao J, Zhang K. Current hydrogel advances in physicochemical and biological response-driven biomedical application diversity. Signal Transduct. Target. Ther. 2021;6(1).
[12] Tsimberidou AM, Fountzilas E, Nikanjam M, Kurzrock R. Review of precision cancer medicine: evolution of the treatment paradigm. Cancer Treat Rev 2020;86: 102019.
[13] Shokri R, Fuentes-Chandía M, Ai J, Habibi Roudkenar M, Reza Mahboubian A, Rad Malekshahi M, et al. A thermo-sensitive hydrogel composed of methylcellulose/ hyaluronic acid/silk fibrin as a biomimetic extracellular matrix to simulate breast cancer malignancy. Eur Polym J 2022;176:111421.
[14] Norouzi M, Nazari B, Miller DW. Injectable hydrogel-based drug delivery systems for local cancer therapy. Drug Discov. Today 2016;21(11):1835–49.
[15] Feng D, Bai B, Wang H, Suo Y. Enhanced mechanical stability and sensitive swelling performance of chitosan/yeast hybrid hydrogel beads. New J Chem 2016; 40(4):3350–62.
[16] Li D, Wang S, Meng Y, Guo Z, Cheng M, Li J. Fabrication of self-healing pectin/ Chitosan hybrid hydrogel via Diels-Alder reactions for drug delivery with high swelling property, ph-responsiveness, and cytocompatibility. Carbohydr Polym 2021;268:118244.
[17] Bashir S, Omar FS, Hina M, Numan A, Iqbal J, Ramesh S, et al. Synthesis and characterization of hybrid poly (N, N-dimethylacrylamide) composite hydrogel electrolytes and their performance in Supercapacitor. Electrochim Acta 2020;332: 135438.

[18] Aston R, Sewell K, Klein T, Lawrie G, Grøndahl L. Evaluation of the impact of freezing preparation techniques on the characterisation of alginate hydrogels by cryo-SEM. Eur Polym J 2016;82:1–15.
[19] Lin YY, Lu SH, Gao R, Kuo CH, Chung WH, Lien WC, et al. A novel biocompatible herbal extract-loaded hydrogel for acne treatment and Repair. Oxid Med Cell Long 2021;2021:1–13.
[20] Seo JW, Shin SR, Lee MY, Cha JM, Min KH, Lee SC, et al. Injectable hydrogel derived from Chitosan with tunable mechanical properties via hybrid-crosslinking system. Carbohydr Polym 2021;251:117036.
[21] Haung HY, Wang YC, Cheng YC, Kang W, Hu SH, Liu D, et al. A novel oral astaxanthin nanoemulsion from haematococcus pluvialis induces apoptosis in lung metastatic melanoma. Oxid Med Cell Long 2020;2020:1–13.
[22] Khan AH, Smith NM, Tullier MP, Roberts BS, Englert D, Pojman JA, et al. Development of a flow-free gradient generator using a self-adhesive thiol-acrylate microfluidic resin/hydrogel (TAMR/h) hybrid system. ACS Appl Mater Interfaces 2021;13(23):26735–47. [23] Hu Y, Kim Y, Jeong J, Park S, Shin Y, Ki Hong I, et al. Novel temperature/ph- responsive hydrogels based on succinoglycan/Poly(N-isopropylacrylamide) with improved mechanical and swelling properties. Eur Polym J 2022;174:111308. [24] Akay S, Heils R, Trieu HK, Smirnova I, Yesil-Celiktas O. An injectable alginate- based hydrogel for microfluidic applications. Carbohydr Polym 2017;161:228–34. [25] Chen S, Wang Y, Zhang X, Ma J, Wang M. Double-crosslinked bifunctional hydrogels with encapsulated anti-cancer drug for bone tumor cell ablation and bone tissue regeneration. Colloids Surf B 2022;213:112364. [26] Liparoti S, Speranza V, Marra F. Alginate hydrogel: The influence of the hardening on the rheological behaviour. J Mech Behav Biomed Mater 2021;116:104341.
[27] Pandit N. Loss of gelation ability of Pluronic® F127 in the presence of some salts. Int J Pharm 1996;145:129–36.
[28] Li Y, Fu R, Duan Z, Zhu C, Fan D. Mussel-inspired adhesive bilayer hydrogels for bacteria-infected wound healing via NIR-enhanced nanozyme therapy. Colloids Surf B 2022;210:112230.
[29] Jenkins RW, Fisher DE. Treatment of advanced melanoma in 2020 and beyond. J Invest Dermatol 2021;141(1):23–31.
[30] Cheng L, Lopez-Beltran A, Massari F, MacLennan GT, Montironi R. Molecular testing for BRAF mutations to inform melanoma treatment decisions: a move toward precision medicine. Mod Pathol 2018;31(1):24–38.
[31] Tawbi HA, Schadendorf D, Lipson EJ, Ascierto PA, Matamala L, Castillo Guti´ errez E, et al. Relatlimab and nivolumab versus nivolumab in untreated advanced melanoma. N Engl J Med 2022;386(1):24–34.
[32]Wang S, Li Q, Feng S, Lv Y, Zhang T. A water-retaining, self-healing hydrogel as ionic skin with a highly pressure sensitive properties. J Taiwan Inst Chem Eng 2019;104:318–29.
[33] Nie J, Gao Q, Wang Y, Zeng J, Zhao H, Sun Y, et al. Vessel-on-a-chip with hydrogel-based microfluidics. Small 2018;14(45).
[34] Chen WY, Matulis D, Hu WP, Lai YF, Wang WH. Studies of the interactions mechanism between DNA and silica surfaces by isothermal titration calorimetry. J Taiwan Inst Chem Eng 2020;116:62–6. [35] Lee IC, Chang JF, Juang RS. Recent advances and perspectives on capture and concentration of label-free rare cells for. Biomed Sci Eng Res J Taiwan Inst Chem Eng. 2018;85:40–55.